Phase characterization of polarimetric SAR images

Matteo Soccorsi[a] and Mihai Datcu[a,b]

[a]German Aerospace Center, Remote Sensing Technology Institute,
Oberpfaffenhofen, 82234 Weßling, Germany;
[b]Télécom Paris, 46 rue Barrault, 75013 Paris, France

ABSTRACT

High Resolution (HR) Synthetic Aperture Radar (SAR) Single Look Complex (SLC) observations, mainly of strong scattering scenes or objects show phase patterns.
Phase patterns may occur due to the *system* behavior or they may be *signatures* of the imaged objects. Since state of the art stochastic models of SAR SLC data describe mainly the pixel information. Now studies are needed to elaborate better models for the full information content. Thus, new statistical models of HR SAR SLC are proposed, they aim at the characterization of the spatial phase feature of Polarimetric SAR (PolSAR) SLC data, i.e. they describe multi-band, complex valued textures.

The definition of texture must be changed because it is not anymore characterizing the optical features but the electromagnetic properties of the illuminated targets.
The content of the SAR image is a stochastic process characterized from its own structure and geometry, which differs from the real one of the illuminated scene, and is dominated from strong scatterers.
Nevertheless we are going to accept the classical texture definition, inherited from computer vision, in homogeneous areas and, furthermore, we are going to extend it for a characterization of isolated and structured objects The proposed models are in the class of simultaneous Auto-Regressive (sAR) defined on a generalized set of cliques in the pixel vicinity.
Models may have different orders, thus capturing different degrees of the data complexity. To cope with the problem of estimation and model order selection Bayesian inference is used.
The results are presented on PolSAR data.

Keywords: Feature extraction, texture, GMRF, PolSAR, SLC

1. INTRODUCTION

Synthetic Aperture Radar (SAR) signals contain information which describes objects and structures of the illuminated scene. On the other hand, object and structure recognition in SAR is not a straight task.
The image interpretation is not easily carried out by not expert users, thus, more automated tools are needed for the interpretation of SAR images.

The task is to find a robust parametrical representation of the signal in order to use the estimated parameters as descriptors of the scene content. Through the combination of parameters (or primitive feature) we want to be able to describe the textures characterizing the scene.
Although we have applied a classification method, our final purpose is not image classification or segmentation, thus we use the unsupervised classification, as a vector quantization, to assess the goodness of the estimated parameters.
The statistical modeling allows a compact description of the signal through the estimation of significant parameters, whereas the Bayesian approach provides a direct method for parameter estimation and model comparison. The statistics of multilook polarimetric and inteferometric SAR image are derived in,[1] where the probability density functions (pdfs) of the multilook phase differences, magnitudes of complex products, and intensity and

Further author information: (Send correspondence to M.S.)
M.S.: E-mail: matteo.soccorsi@dlr.de, Telephone: +49 (0)8153 28 3302
M.D.: E-mail: mihai.datcu@dlr.de/mihai.datcu@enst.fr, Telephone: +49 (0)8153 28 1388/+33 (0)1 45 81 72 88

amplitude ratios are investigated. On the other hand, the statistical characteristics of multilook data are different from those of single-look data.

We propose an extension of the Gauss-Markov Random Field (GMRF) model in the complex domain for complex-valued data, and We introduce a GMRF model for complex-valued multi-band data.
We want to exploit the full information contained in the scene signal, i.e. amplitude and phase.

The results are presented on Polarimetric SAR (PolSAR) data acquired over the city of Mannheim, Germany. A compared analysis of the best band order is also provided.

2. SAR SIGNALS

High Resolution (HR) Synthetic Aperture Radar (SAR) images are bi-dimensional complex signals and reveal structures both in amplitude and phase as shown in Fig. 1, where three examples of texture are presented in the form of amplitude (top row) and corresponding phase image (bottom row). The first example, Fig. 1(a), shows a quasi-uniform backscattering from a vegetated area with no phase structure, Fig. 1(d). The second one, Fig. 1(b), shows distributed scatterers with no phase structure again, Fig. 1(e). The last example, Fig. 1(d), shows very strong combined scatterers, and the phase image reveals a correlation pattern, Fig. 1(f).
HR SAR image texture must be redefined because it is not any more characterizing optical features, but, in contrast, electromagnetic properties of the illuminated targets. This basically distinguishes optical from SAR images and makes the interpretation of the latter a difficult task, because what SAR image formation and acquisition record is different from visual perception.
The content of a SAR image is characterized by its own geometry, which differs from the real geometry of the illuminated scene and is dominated by strong scatterers. Nevertheless, we are going to accept the classical texture definition in homogeneous areas, but we are going to extend it for a characterization of isolated and structured objects.
Since the task in SAR is to detect and recognize objects and structures, we redefined the texture as a local descriptor of the scatterers and structured scatterers. The contextual information is the spatial descriptor in the vicinity of each pixel. Thus, texture information is a descriptor of the scene structures and objects, to be extracted as texture parameters, which are a fingerprint of the local structure and a feature for classification of different textures and for object recognition.

On the other hand the Polarimetric SAR (PolSAR) data are even more complicated signal because each pixel in the image is represented by a four dimensional complex vector. An example of PolSAR data is shown in Fig. 2, where three of the four polarimetric channels are given together with the complex data format (real and imaginary channels). Each band captures different polarimetric characteristics of the data.
A significant example is given in Fig. 3. The river area (color coded), Fig. 3(a), presents a phase pattern, Fig. 3(b). The complex-valued GMRF is able to model the phase pattern as shown in the model evidence in Fig. 3(c), where the higher evidence corresponds with the areas in which the phase patterns appear.
It is still not clear what can produce these patterns in the acquired image and why they appear in a really noisy area, e.g. the river.

3. IMAGE MODEL

The classical image model for SAR data is the circular complex Gaussian model, which is ensured in the hypothesis of fully developed speckle, i.e. a large number of scatterers in the resolution cell. The non-linear transformation from cartesian to polar coordinates brings to a negative exponential distribution for the image intensity and a uniform distribution for the phase.
As demonstrated in[2] the hypothesis of fully developed speckle drops in High Resolution (HR) SAR images. Thus we need more appropriate models to fit the data and capture the characteristics of the SAR signal. Thus we propose a GMRF model for complex-valued data.

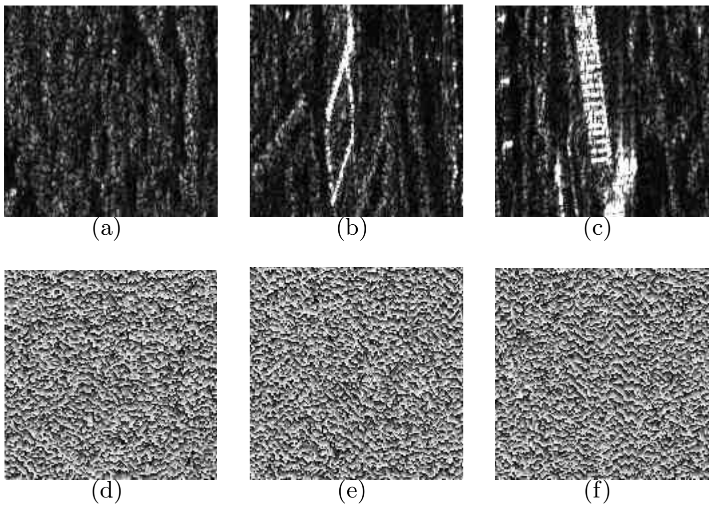

Figure 1. Texture examples from a HR SAR image. Amplitude image (top row) and corresponding phase (bottom row). The first example (a) shows a quasi-uniform backscattering from a vegetated area with no phase structure (d). The second one (b) shows distributed scatterers with no phase structure again (e). The last example (d) shows very strong combined scatterers, and the phase image reveals a correlation pattern (f) which is visible in azimuth as an ensemble effect of the strong scatterer side lobs.

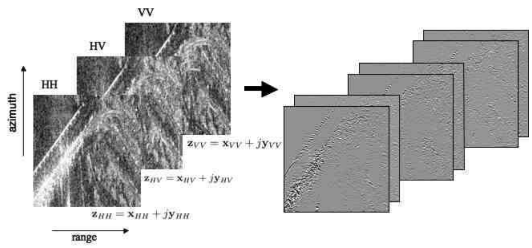

Figure 2. Example of PolSAR images and signals. Three polarimetric bands HH-HV-VV representing the stack of analyzed data. Each band is characterized by a complex signal composed by real and imaginary channels. On the right side is visible the stack of complex data. The SAR signal is not easy to interpret.

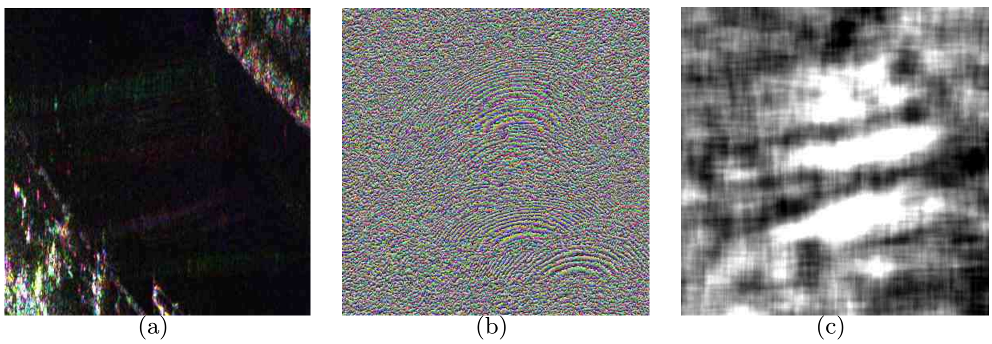

Figure 3. Significant example from the processed tail. The RGB river area (a), the RGB phase image (b), and the model evidence (c). The model evidence is higher over the phase pattern. We want to point out that the image in (b) is a phase image and not an interferogram. The estimation was computed on normalized amplitude.

3.1 Complex-valued Gauss-Markov Random Field

We suppose the texture of the SAR image to be modeled by the model[3] extended in complex domain and given by:

$$z = x + jy, \tag{1}$$

$$\eta_x = \eta_y = 0, \tag{2}$$

$$\sigma_x = \sigma_y = \sigma, \tag{3}$$

$$\theta = \xi + j\tau, \tag{4}$$

$$p(z_s|z_{s+r}, r \in \mathcal{N}) = \frac{1}{2\pi\sigma^2} \exp\left\{ - \frac{\left(\begin{bmatrix} x_s \\ y_s \end{bmatrix} - \sum_{r\in\mathcal{N}} \begin{bmatrix} \xi_r & -\tau_r \\ \tau_r & \xi_r \end{bmatrix} \begin{bmatrix} x_{r+s} \\ y_{r+s} \end{bmatrix} \right)^2}{2\sigma^2} \right\}, \tag{5}$$

where z is the realization of the complex-valued pixel given by the realization of the real and imaginary channels. The condition given by Eq. (2) is ensured by a preprocessing step and the condition of Eq. (3) is a property of the complex random variable z.
The model is a parametrized bivariate Gaussian. The number of elements in the sum is defining the complexity of the model.

3.2 Complex Auto-Regressive process

The argument of the exponential in Eq. (5),

$$\begin{bmatrix} n_x \\ n_y \end{bmatrix} = \begin{bmatrix} x_s \\ y_s \end{bmatrix} - \sum_{r\in\mathcal{N}} \begin{bmatrix} \xi_r & -\tau_r \\ \tau_r & \xi_r \end{bmatrix} \begin{bmatrix} x_{r+s} \\ y_{r+s} \end{bmatrix}, \tag{6}$$

is a complex-valued autoregressive process.
We can write Eq. (6) in the following compact matrix form

$$\mathbf{z} = \mathbf{G}\boldsymbol{\theta} + \mathbf{n}, \tag{7}$$

where $\mathbf{z}$, $\mathbf{G}$, $\boldsymbol{\theta}$, $\mathbf{n} \in \mathbb{C}$. $\mathbf{z}$ is a column vector with the image pixel in lexicographic order, more in detail the vector elements are the pixels belonging to the local analyzing window chosen for the analysis. $\boldsymbol{\theta}$ is the complex-valued parameter vector which number of elements depends on the model order complexity, i.e. the number of defined cliques. $\mathbf{G}$ is the clique matrix which number of rows equals the number of the element of the vector $\mathbf{z}$, whereas the number of columns equals the number of the element of the vector $\boldsymbol{\theta}$. Eventually, $\mathbf{n}$ is the stationary complex Gaussian noise.
Equation (7) is an over-determined linear equation system, which can be solved by a complex Least Square Estimation

$$\hat{\boldsymbol{\theta}} = \left(\mathbf{G}^H\mathbf{G}\right)^{-1}\mathbf{G}^H\mathbf{x}, \tag{8}$$

where $\cdot^H$ is the Hermitian operator and $\hat{\boldsymbol{\theta}}$ is the estimated parameter vector.

4. EXPERIMENTAL RESULTS

The model allows a subjective definition of number and structure of the clique to study, analyze and capture the pixel vicinity features. In order to fit the model with multi-band data we define a system of cross-band cliques. In a 3D pixel disposition, in the simplest case and considering a symmetrical structure, we can estimate three parameters for a model of first order complexity and nine parameters for a model of second order complexity. Whereas to define higher model order is possible if the proper number of bands is available.

Thus, we applied the simultaneous AR (sAR) estimator on the PolSAR data for model order two.
As further analysis than the one presented in,[4] we applied the estimator on different band arrangements, because

the central band is taken as reference. Thus, in order to have a full data analysis we have to extract the spatial feature with all the possible band dispositions.

We analyzed a representative tail (1024×1024 pixels) acquired over the city of Mannheim, Germany, Fig. 4(a).
The data are E-SAR L band with a resolution of 1.20 m in azimuth and 1.99 m in range. In the processing chain we neglected the VH band in the hypothesis of reciprocity, the difference between the bands HV and VH is given only by the thermal noise.
We analyzed the data with an Analyzing Window (AW) of 35×35 to ensure enough number of samples for the estimation and the data are supposed to be homogenous in the AW.
The limit of the size of the analyzing window with the spatial diversity and the edges effects were not taking into account in this preliminary results. By the way, for a purpose of classification preprocessing steps (e.g. edge detection, despeckling) can be introduced to ameliorate the results.

We are interested in the separation of different textures contained in the image and the classification is only a medium to assess the quality of the estimated parameter.
Specifically, we want to asses the best bend data arrangement with the current analysis, thus we compare the histograms of the Log-Evidences, Fig. 5(d).

The original color coded image with the model evidence and the amplitude of the vertical and horizontal cross-band cliques are shown in Fig. 4. The model evidence shows grater values where the model fits better the data. The vertical and horizontal cross-band cliques are characterizing different data behavior.
The parameters were estimated for three different band orders, HH-HV-VV, HV-VV-HH, and HV-HH-VV. The evidence of the model which has inside the information collected by the estimated parameters was classified. The results of the unsupervised classification, based on the evidence, are shown in Fig. 5.
In the absence of a ground truth, we can give a qualitative meaning to the classes. The five classes, within the limit of the sensor resolution and the analyzing window size, correspond to water (light blue), non-built area (yellow and blue), residential area (green), and big buildings and strong scatterers (red).
The classifications appear similar but there are small differences in the classes, especially red and green which made more accurate the results obtained for the HV-HH-VV order of bands.
The histograms of the Log-Evidence 5(d) confirms the classification results. The color lines correspond to the probability density function (pdf) of the Log-Evidence for HH-HV-VV (black line), HV-HH-VV (red line), and HV-VV-HH (blue line).
The histogram, corresponding to HV-HH-VV (red line), confirms that the better classification is due to the more discernible peaks in the high value of the evidence.
From a Bayesian perspective, the data arrangement which best fits the model is HH-HV-VV, because The Log-Evidence (black line) shows higher values.

5. CONCLUSION

The paper presents the application of a complex-valued GMRF on multi-band PolSAR data. The model is exploiting the amplitude, the phase, the polarimetric and the spatial information. By a 3D system of cliques have been analyzed a representative image from an E-SAR L band scene acquired over the city of Mannheim, Germany.
In the 3D system of clique definition the order of band is important because the central band is taken as reference. Thus we perform an analysis of the best band order disposition.
The model parameter evidence unsupervised classification reveals that the classes are more accurately representing the content of the image in the case of HV-HH-VV band order disposition. However, from a Bayesian point of view, the optimal bend arrangement is HH-HV-VV because the histogram shows higher values than the others.
Nonetheless, we have to consider that this is a data depend result and another data set can give different results. Further work an analysis have to be performed, because this is only a preliminary results for a full polarimetric complex signal modeling approach. The complexity of the SAR data signals is really high and the information content have to be accurately modeled.
A next step will be the development of a fully polarimetric multivariate AR process in order to find the complete

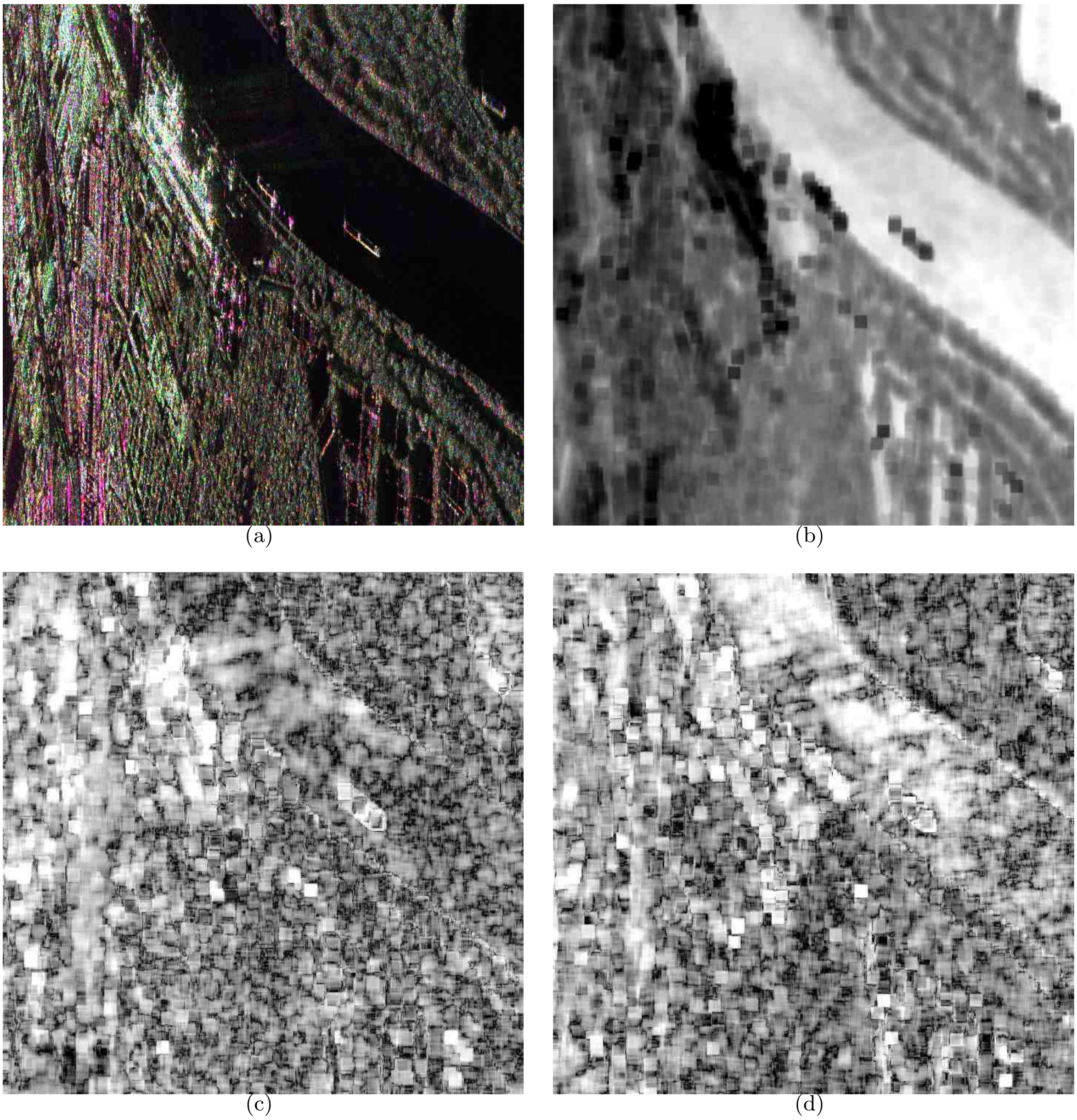

Figure 4. Polarimetric color coded E-SAR L band image (azimuth resolution 1.20 m, range resolution 1.99 m) (a). Example of model evidence (b). Amplitude of the vertical and horizontal cross band cliques (c) and (d). The image was chosen for the strong content variability. There are representative classes of water, vegetation, residential area, and big buildings. The evidence of the model is a measure of how good the model fits the data. The higher value of the evidence is obtained for the class water, where the signal to noise ratio is supposed to be very low. The vertical and horizontal parameters as well as all the other estimated parameters are capturing the spatial behavior of the analyzed data.

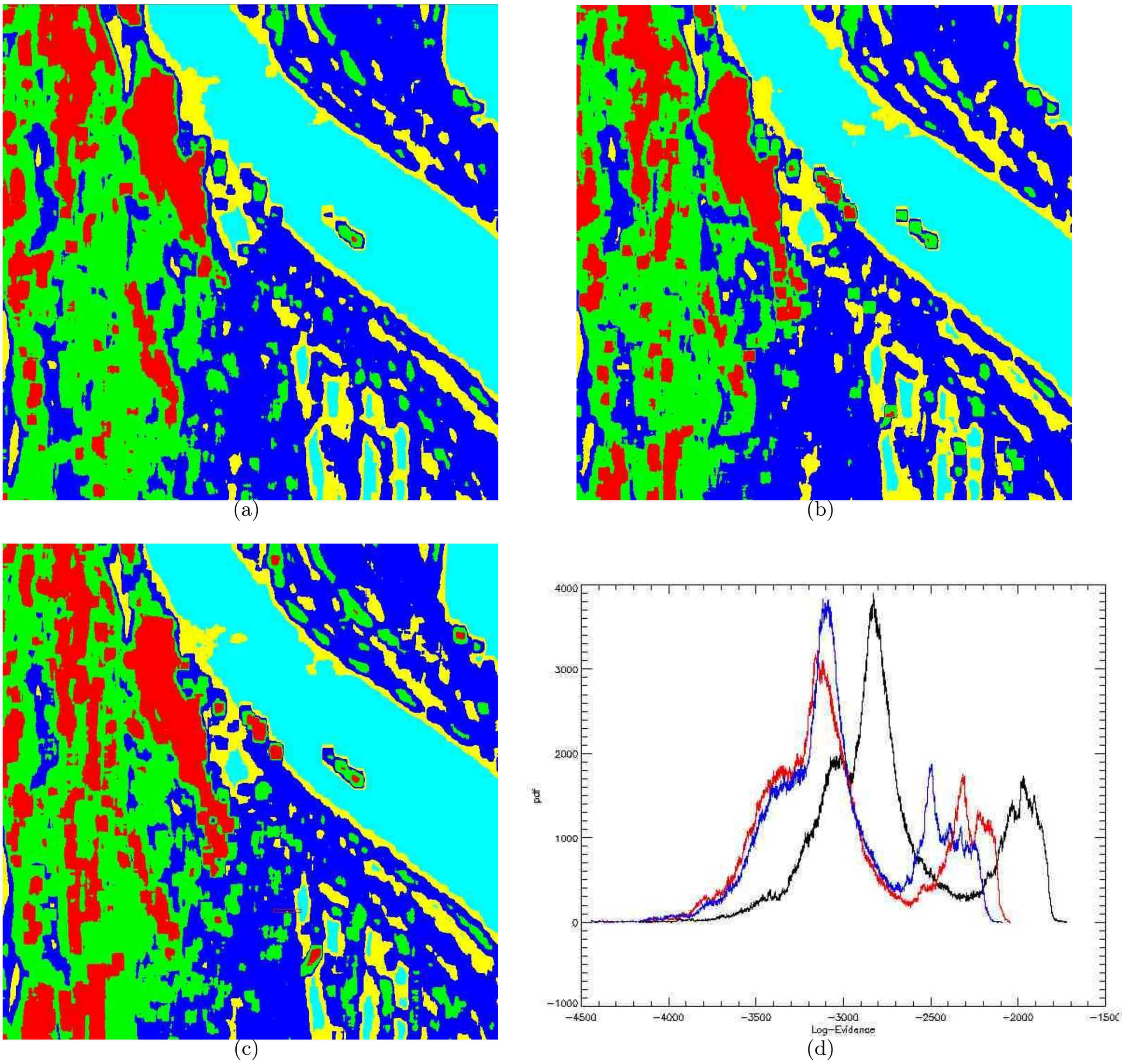

Figure 5. Unsupervised classification based on the model evidence for different band dispositions: HH-HV-VV (a), HV-VV-HH (b), and HV-HH-VV (c). The five classes correspond to water (light blue), non-built area (yellow and blue), residential area (green), and big buildings and strong scatterers (red). Probability density function (pdf) of the Log-Evidence (d) for HH-HV-VV (black line), HV-HH-VV (red line), and HV-VV-HH (blue line). The classifications appear similar but there are differences in the classes, especially red and green which made more accurate the results obtained for the HV-HH-VV order of bands. The histogram behavior, corresponding to HV-HH-VV (red line) confirms that the better classification is due to the more discernible peaks in the high value of the evidence. From a Bayesian perspective the model which fits better the data is the one with the higher evidence.

spatial information delivered by PolSAR data. The analysis performed by this extended model is supposed to be independent from the band order.
The comparison of this approach with the information contained in the Wishart distribution will be investigate. Furthermore, new methods for the assessment of the parameters, e.g. measure of the information content, distance measures, etc., will be explored in order to give a full justification to the method.
The results will be helpful to speed up the development of Image Information Mining system, e.g. Knowledge based Information Mining (KIM) system,[5] and to prepare the TerraSAR-X ground segment. Possible applications are automatic detection, recognition, classification, and scene understanding.

ACKNOWLEDGMENTS

This work was carried out in the frame of the *CNES/DLR/ENST Competence Center on Information Extraction and Image Understanding for Earth Observation*. The authors would like to thank Gottfried Schwarz for his helpful hints.

REFERENCES

1. J.-S. Lee, K. W. Hoppel, S. A. Mango, and A. R. Miller, "Intensity and phase statistics of multilook polarimetric and interferometric SAR imagery," *IEEE Transaction on Geoscience and Remote Sensing* **32**, pp. 1017–1028, September 1994.
2. D. Petit, L. Soucille, J.-D. Durou, F. Adragna, H. Oriot, and E. Simonetto, "Spatial phase behavior in SAR images," in *SAR Image Analysis, Modeling, and Techniques IV*, F. Posa, ed., *Proc. SPIE* **4543**, pp. 53–63, 2002.
3. R. Chelappa, S. Chatterjee, and R. Bagdazian, "Texture synthesis and compression using Gaussian-Markov Random Field models," *IEEE Transaction on Systems, Man, and Cybernetics* **15**, pp. 298–303, March/April 1985.
4. M. Soccorsi and M. Datcu, "Stochastic models of SLC HR SAR images," *Proc. IGARSS*, 2007.
5. M. Datcu, H. Daschiel, A. Pelizzari, M. Quartulli, A. Galoppo, A. Colapicchioni, M. Pastori, K. Seidel, P. G. Marchetti, and S. DElia, "Information mining in remote sensing image archives - Part A: System concepts," *IEEE Transaction on Geoscience and Remote Sensing* **41**, pp. 2923–2936, December 2003.